

THE NUMERICAL SIMULATION AND EXPERIMENTAL VALIDATION OF VENTILATION FLOW AND FIRE EVENTS IN A TRENT NACELLE FIRE ZONE

A.J. Mullender and M.H. Coney
Rolls-Royce plc, P.O. Box 31, Derby, UK

D.M.Horrocks
CPS, Universidad de Zaragoza, LITEC, Maria de Luna, 3, 50015, Zaragoza, Spain

J.J.McGuirk
Department of Aeronautical and Automotive Engineering and Transport Studies,
Loughborough University, Leicestershire, UK

J.B.Moss, P.A.Rubini, C.D.Stewart and D.Binks
School of Mechanical Engineering, Cranfield University, Bedford, UK.

Keywords: *engine, fire, ventilation, certification.*

Abstract

Design for aircraft engine zone ventilation and fire certification has traditionally been driven by practical demonstration using standardised tests. For large structures in particular, the cost of carrying out such tests can become prohibitively expensive. Numerical simulation provides the opportunity to investigate structure and component performance both during normal operation and in the event of fire and thereby promote greater integrated design.

One of the major problems in any numerical simulation of a complex geometrical system is obtaining a suitable representation of the geometry to be used in the simulation process - in this case structured and unstructured grid generation and Computational Fluid Dynamics (CFD) analysis. With current Computer Aided Design (CAD) practises, the geometry is not in a suitable form and with large datasets such as those used here, the problems are often exacerbated. The challenges associated with the identification of

a suitable geometry subset from the full engine assembly tree, filtering of unusable detail and additional CAD preparation for the grid generation are addressed. The realisation of tractable but representative geometries is illustrated by examples characteristic of the Trent engine family.

The numerical simulations focus on the capture of the key physical processes. During normal operation this encompasses the ram inlet zone ventilation flow, including heat transfer from engine casings and accessories, whilst for a fire event this will additionally include the interaction with the buoyantly driven fire plume. The scenario investigated in this paper is that of a burner-simulated gearbox fire. Predictions of the internal velocity field, gas temperatures and composition and wall heat fluxes are compared with experimental measurements on a ½ scale nacelle fire test rig and, for the ventilation flow, with visualisation using dye and bubble tracers in a Perspex model of similar scale by water analogy. The numerical simulations capture important features of this complex flowfield and are shown to identify a number of distinct opportunities for design refinement.

1 Geometry Capture

1.1 Objective

To determine the feasibility of performing production type simulations of the ventilation flow and heat transfer in typical Trent engine fire zones, using the full Electronic Product Definition (EPD) of the geometry as the starting point.

1.2 Introduction

In keeping with modern concurrent engineering practices, there should only be a single definition of the geometry used to describe the current design condition of any component in a large assembly. There can be many different instances of this geometry, that are possible alternative designs, but again, there should only be one geometric definition of each instance. In a project as large, and with as many dependencies as a complete aeronautical gas turbine engine, the need for this centralisation of data is obviously imperative. However, the level of geometric detail that is necessarily stored for a part design is not always required, or even suitable for use in the various numerical (and experimental) studies that need to be performed in order to gauge the performance of each individual part, or the assembly as a whole. These studies will often need to use a subset, or some simplified geometrical representation of the actual geometry to enable reasonable predictions to be obtained within the constraints of the computing power, or experimental measuring techniques available.

1.3 Method

The supplied geometries came in the form of full Computervision CADDSS5 Concurrent Assembly Mock Up (CAMU) engine assemblies (see

Figure 1 – Trent 800 Zone 1 and

Figure 2 - Trent 500 Zone 1 and Zone 3).

The assembly shown in

Figure 1 was composed of approximately seven hundred individual part files, some defined by Rolls-Royce, others by the various sub-contractors, and took nearly 15Gb of disk

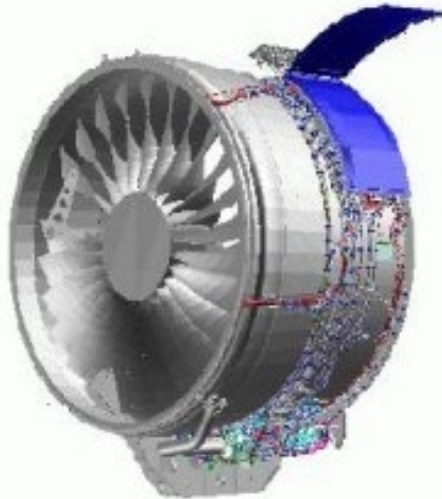


Figure 1: Trent 800: zone 1 (external to fancase)

space. At the outset of the project, it was not clear regarding which components were actually going to be of interest in the aerodynamic study to be performed. As such, the identification of these components was one of the first problems to be tackled. The Computervision Optegra suite of software was used in helping to determine which parts were deemed to be important to the study. This software allowed 'fly-throughs' of very large geometries to be performed, and important information such as the relative locations, clearances, corresponding CADDSS5 part file etc. could be extracted through this process. It allowed the (obviously highly subjective) identification of components of interest in the zones to be performed.

Having identified these components, it was then possible to create a single, but still large (of the order 300Mb) CADDSS5 part file that contained the design geometry of all of the components that were deemed important enough to include in the initial numerical studies. There was obviously far too much geometric detail for any downstream numerical analysis to be able to deal with, so a geometry of reduced complexity, which was still representative of the part being modelled needed to be created.

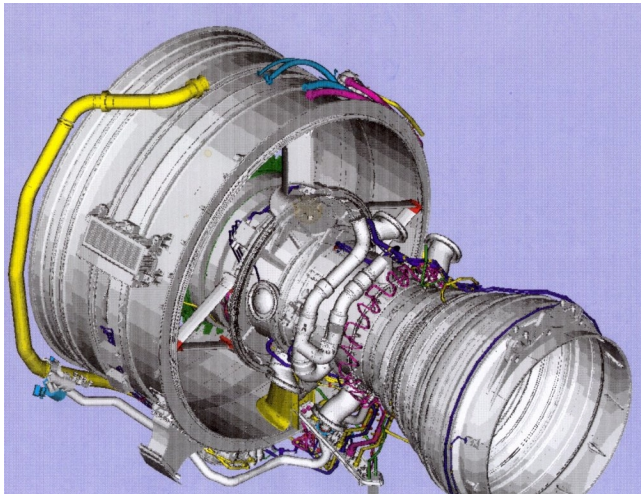


Figure 2: Trent 500 - port view

This meant that each individual component identified had to be manually filtered of all detail that was considered either unnecessary (in the context of the resolution of the study) or unmanageable in the downstream grid-generation and subsequent numerical solution (see Figure 3 and Figure 4).

A solid model of the fluid volume in the zone, generated from the solids defining the components, and closing all inlet and exit planes to the zone was required as the geometric input to the grid-generator. It should be noted that the geometry identification and subsequent filtering required in order to get a model that was of high enough integrity, but low enough complexity in order for the numerical analysis to proceed took well over fifty percent of the total time required by the study, from receiving the initial geometry data to obtaining a CFD prediction.

Having obtained a suitably manageable but representative geometry, it was necessary to generate the grids to be used in the study. The Fluent suite of software was used, and in order for the CADDSS5 geometry to be imported into the Fluent environment, a neutral IGES file of the geometry was created in CADDSS5, which could then be read by the geometry (surface) modeller (called DDN) used by Fluent.

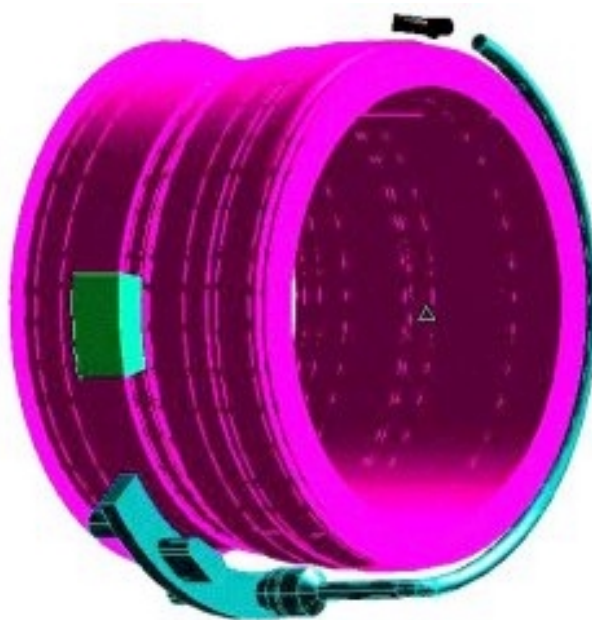


Figure 3: Starboard view of inner casing of filtered geometry – Trent 800 zone 1

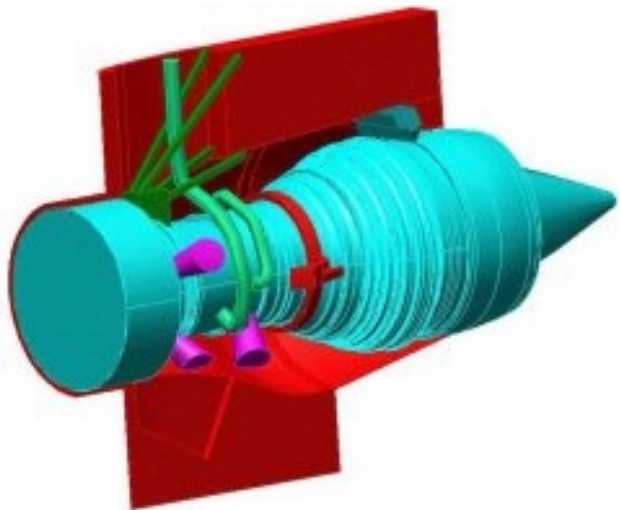


Figure 4: Cutaway view of filtered Trent 500 zone 3 geometry

Unstructured grid generation generally proceeds in two stages - the first stage being the generation of a 2D surface mesh on the boundary of the computational domain (the fluid volume). The internal grid (the volume mesh) is then generated from this boundary mesh. Since the geometry for each fire zone being used in this study were very large (i.e. consisted of a large number of geometry regions), it was decided at the outset to split the

geometry used to define the boundary into a number of different portions, and to then generate the surface grid for each of these portions separately. Once all of these subsets of the surface geometry had been gridded, it was then possible to merge them all together to form the 2D boundary mesh for the whole of the closed surface bounding the computational domain. The decomposition of the geometry into these smaller surface portions was achieved through the rigorous use of levels (or layers) in the geometry modelling, which meant that only the uncluttered geometry of interest was displayed and used at any one time. This process meant that a fair amount of time was spent in ensuring that adjacent portions of this decomposed surface grid had a matching node distribution along the common edges between each grid. Another small overhead was introduced by this process, as some of these grid portions still needed to be manually merged once they were butted together to form the whole surface grid. However, this splitting up of the surface geometry meant that each portion of the boundary grid was relatively simple to grid, since visualization of the geometry was significantly easier and large gains in performance of the software used to generate the surface meshes (Geomesh) were had. As such, it was felt that the initial decision to decompose the surface grid was justified.

When generating the surface grids for each decomposed portion, extensive use was made of the fact that some of the engine casings could be treated as surfaces of a volume of revolution. The quality of the surface mesh is reduced by the presence of highly skewed cells - the implication of this is that for a good quality surface mesh, reasonably equilateral elements are required. This is not easy to achieve on regions of high aspect ratio, such as fins or castellations in the geometry surfaces. However, if a small section, say 45 degrees, of a rotationally symmetrical surface is taken, then it is not too difficult to obtain a grid that is not unduly skewed on this portion (see Figure 5).



Figure 5: Surface mesh on a 45 degree section of a body of revolution (Trent 500 zone 3)

The grid on this section can then be copied and rotated around the full 360 degrees of the geometry, then merged together, thus defining a surface mesh of acceptable quality over these high aspect ratio, but still important regions in the geometry (see Figure 6). The one drawback of this is that there is generally only one or two boundary cells along the shortest dimension of the high aspect ratio regions, and the resolution may be excessive along the longest dimension.



Figure 6: Annular surface mesh obtained by rotating the surface mesh above

The spacing of the nodes positioned along the edges of the surfaces used to generate the boundary mesh is dictated by three factors. Firstly, it needs to be sufficient to capture the geometric features of the surface it is on. Secondly, it needs to be sufficient to enable a surface grid of acceptable quality to be generated (i.e. not too highly skewed). Thirdly, it needs to be of a suitable spacing so that the volume mesh generated from this resulting boundary mesh is also of an acceptable quality. In areas of the domain where there are thin gaps between surfaces for example, a coarse node spacing may give a smooth, equilateral surface mesh of very high quality. However, the generation of a volume element (tetrahedron) of similar quality will not be able to be achieved, only very 'squat' tetrahedra can be generated, which are of very poor quality.



Figure 7: Surface mesh on the inner wall of Trent 800 zone 1

Some of the surfaces that have been used to create the geometry regions are quite complex - for example, the highly curved inner lining of the nacelle, and some intersecting pipe-work. When generating the surface meshes on these regions, it is necessary to project the nodes of the mesh onto the geometry. This will only be successful if the original geometry (generated in CADD5) is of high quality. Once the surface mesh portions have been merged together, there is often some time needed to be spent to ensure that the whole surface mesh is of

an acceptable quality before the volume mesh is generated. Since the quality of the volume mesh is heavily dependent on the quality of the surface mesh it is generated from, then any time improving the boundary mesh is time well spent. Edge swapping and Laplacian smoothing can be performed, but there is also a lot of manual repair required (splitting edges, locally repositioning nodes, further swapping of edges, etc.) in order to get a suitable boundary mesh (see Figure 7, Figure 8 and Figure 9).

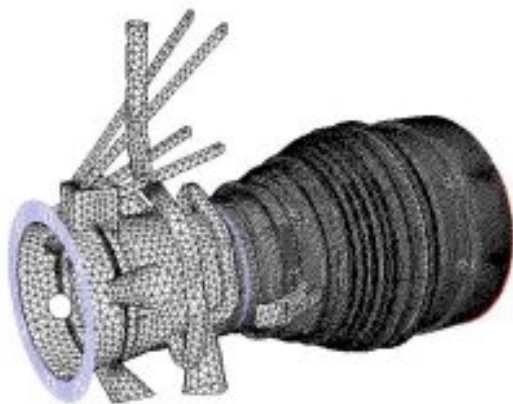


Figure 8: Surface mesh on the inner wall and blockages of Trent 500 zone 3

Once the boundary mesh has been generated and is deemed to be of an acceptable quality, then it is usually a simple task of automatically generating a volume mesh from this. Again, once a mesh has been generated, certain quality checks need to be performed, and if any cells fail these checks, manual grid repairs can be performed (face swapping, node repositioning, etc.). However, if starting from a suitable boundary mesh and one has specified sensible parameters (such as change in cell size between adjacent cells, cell skewness measures, etc.), then the volume mesh should be acceptable for use in the solver.

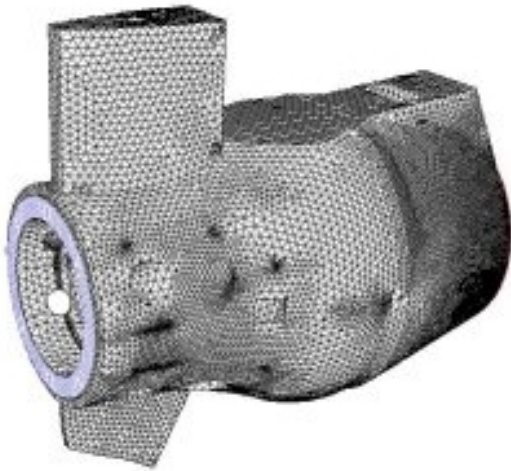


Figure 9: Surface mesh on the outer wall of Trent 500 zone 3

2 The Simulation of Ventilation Flows and Fire Events

2.1 Experimental Rigs

Simplified representations of the fan casing geometry have been incorporated in two, approximately half-scale experimental rigs - a Perspex rig for water analogy flow visualisation (Figure 10) and a water-cooled, mild steel design for fire event simulation (Figure 11 and Figure 12).

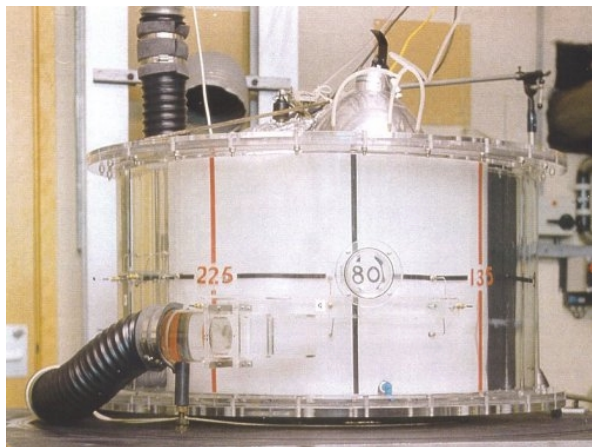


Figure 10: Perspex water rig used for dye injection flow visualisation

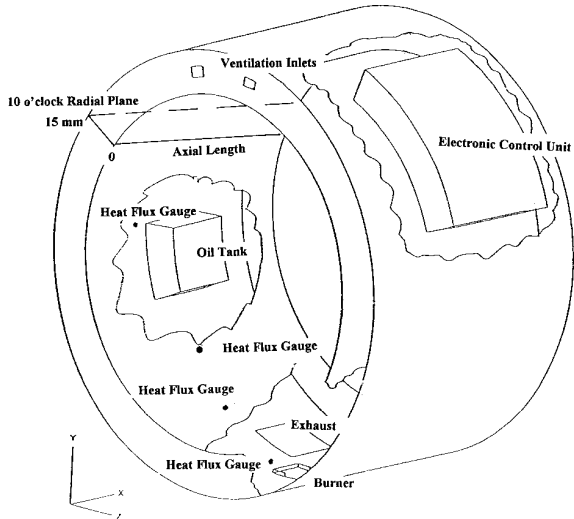


Figure 11: Steel, water cooled fire rig - schematic

Internal complexity in the casing annulus, arising from the electronic control unit, oil reservoir, gearbox, starter motor and air duct, has been introduced progressively in both rigs.

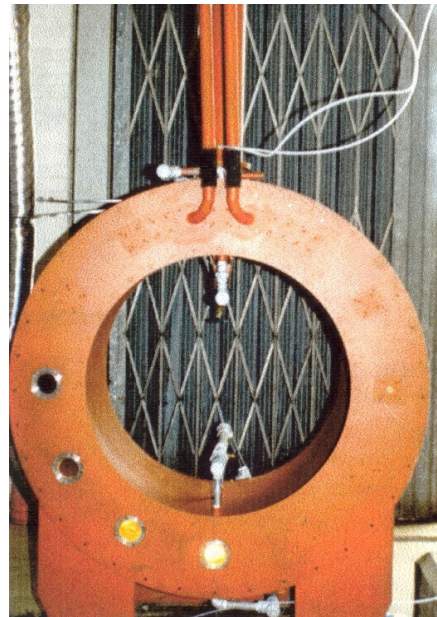


Figure 12: Front view of water cooled fire rig

Sequential dye injection through hypodermic tubes mounted at multiple locations in the Perspex model

Figure 10 permits individual flow features to be clearly distinguished. For example, ventilation jet penetration and interaction with mounted accessories and the eventual mixing of the separate counter-current flows in the vicinity of the gearbox deployed at the bottom of the rig.

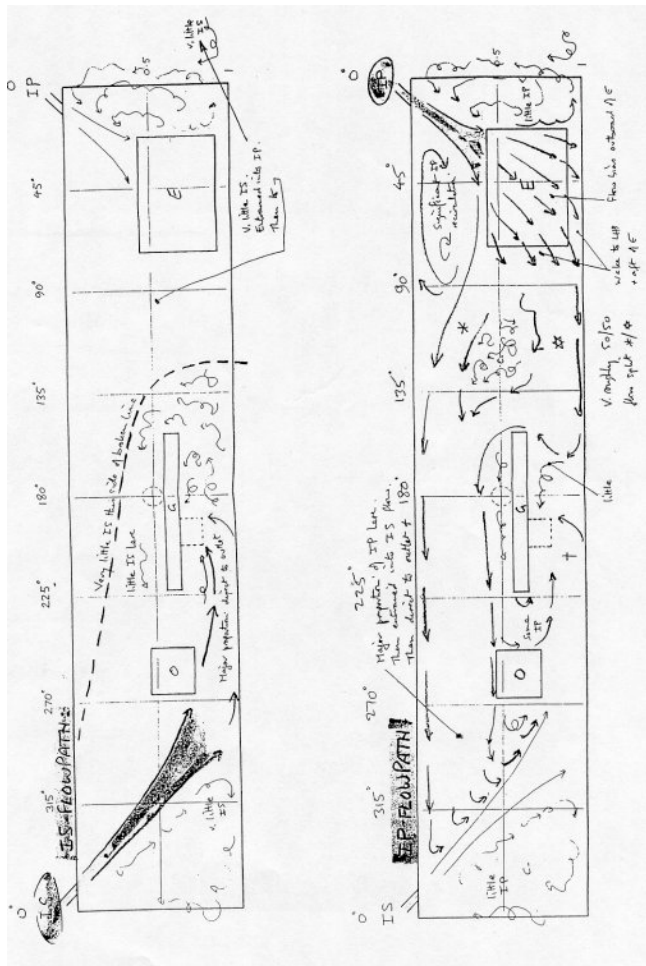


Figure 13: Sketches of flow development from water and dye visualisation

The development of the inert flows in the annulus is sketched in Figure 13, based upon a series of individual dye injection photographs. Whilst detailed quantitative measurements from the water analogy investigation cannot be readily interpreted in terms of ventilation flows in air, the broad aerodynamic features visualised can be compared with the CFD simulations reported later.

The fire simulation rig, a simplified half-scale representation of a Trent 800 casing, comprises inner and outer cylindrical walls of diameters 1220 and 1520 mm respectively, 850 mm in axial length, which are water cooled in order to provide a durable experimental facility. Of the many fire events which might be envisaged, experiments to date have focused on

buoyant fires originating at rig bottom-dead-centre.

A circular burner, 128mm in diameter, is located in the outer drum, mid-way along the cylinder. Gaseous fuel, methane and propane, is discharged at low velocity ($\sim 20 \text{ cms}^{-1}$) into the casing, simulating the steady burning of an evaporating liquid-fuelled pool fire. Heat release rates from the fire ranging from 50-120 kW have been investigated. The annular end-plates are fitted with circular ports at 30° intervals, providing probing access to the casing space for thermocouple temperature and gas analysis measurement and visual observation. In addition to changes in radiation heat transfer from the buoyant fire plume, reflecting the differing sooting propensities of methane and propane, the fuel selection also affects flame stability. The methane flames proved particularly susceptible to circulating combustion products and heat release rates greater than 50 kW could not be stabilised. At this limiting condition, combustion products penetrate beyond the curtain established by the two ventilation jets at rig top-dead-centre and the simulated pool fire is subject to a crossflow of vitiated air. Propane imposed no comparable restriction and heat release rates in excess of 120kW could be readily stabilised; flow conditions at which the luminous flame, and hence local burning, actually extended at least 30° beyond top-dead-centre.

Sample thermocouple measurements from within the casing are illustrated in Figure 14 and Figure 15 for the 120kW propane fire. A lengthy fire plume is found to impinge on the base of the oil reservoir, subsequently passing to the front of the casing and over top-dead-centre. The peak time-averaged temperatures measured in the extended luminous burning zone approach 1200K but are widely distributed in physical space, reflecting the effects of buoyancy on both the mean plume trajectory and its considerable 'flapping'. Levels of temperature fluctuation of order 230K were measured by fine wire thermocouple (50 μm wire diameter). Given the thermal inertia of the thermocouple these must represent substantial under-estimates of the actual levels attained.

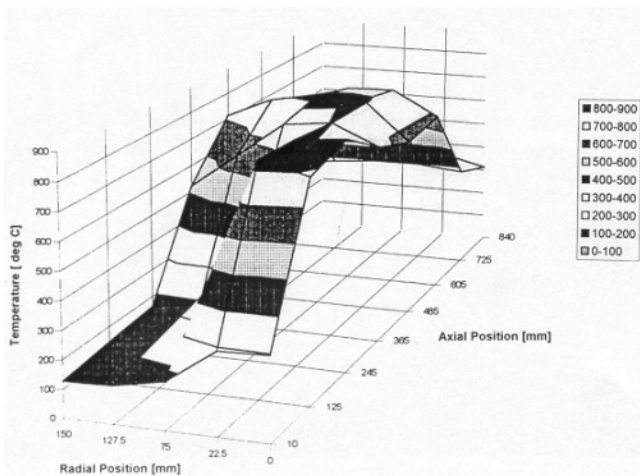


Figure 14: Temperature distribution, 8 o'clock position, 124kW Propane

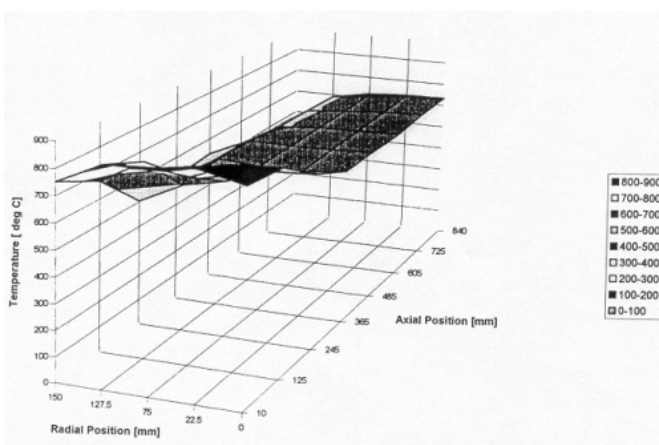


Figure 15: Temperature distribution, 11 o'clock position, 124kW Propane

2.2 Numerical Simulation

Numerical simulation of ventilation flows and fire events has been performed using CFD for both the rig configuration and the more complex geometry of the actual engine casing, derived from a CADDS-based solid model for the Trent 500. Both structured and unstructured meshes have been investigated.

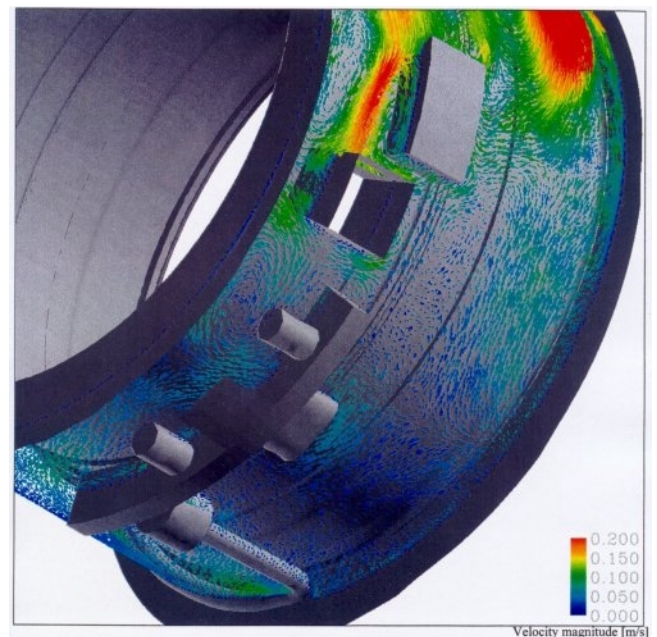


Figure 16: Typical ventilation flow pattern - FLUENT-UNS prediction

Figure 16 illustrates a typical ventilation flow in the vicinity of the engine gearbox as predicted by the code FLUENT-UNS, employing a mesh of 500,000 cells. In the present context detailed comparisons with experiment are restricted to the simpler rig geometry, however, and it is on this case that we focus here.

Structured mesh calculations have been performed for the rig configuration (Figure 17) under ventilation and fire event conditions using the Cranfield fire code SOFIE (reference 1). The computational domain is meshed with 300,000 nodes, permitting some concentration of mesh density in the immediate neighbourhood of the fire plume. Figure 18 illustrates the predicted isothermal flowfield corresponding to a ventilation rate of 9 volume changes per minute. The qualitative features of the flowfield exhibited by the water analogy experiments (c.f. Figure 13) are reproduced in the numerical simulation.

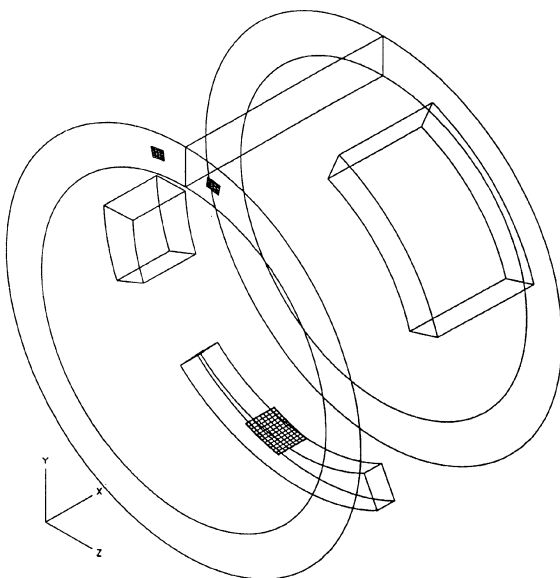


Figure 17: Rig geometry for structured grid numerical simulation

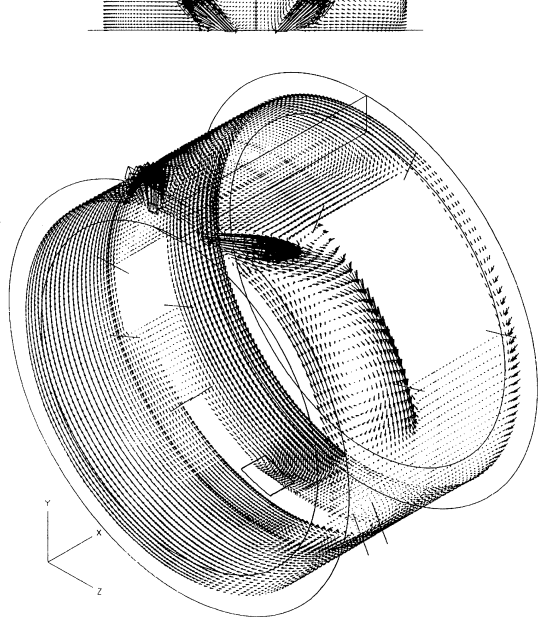


Figure 18: Isothermal flow field for rig geometry at nine zone volumes/ minute flowrate

The impact of the right-hand ventilation jet on the electronic control unit deflects the flow to the front of the rig, whilst that from the left-hand jet passes to the rear of the rig unopposed. Two quite distinct counter-flowing currents are thereby established, with the LH jet passing almost directly to the exhaust port and the RH jet circulating through almost 360° before being entrained by its partner. This underlying flow asymmetry, assisted by the blockage introduced by the gearbox, is then imposed on the buoyant fire simulations and the plume is drawn to the left (c.f. Figure 19). The plume trajectory observed experimentally is fully reproduced by the numerical simulation.

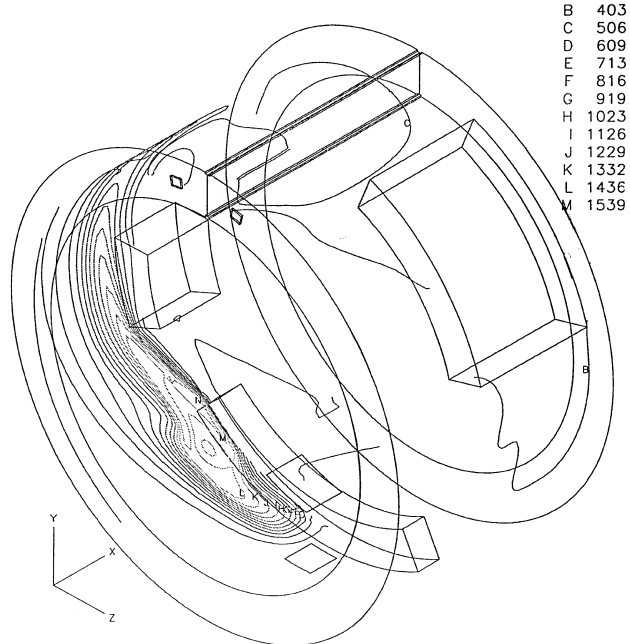


Figure 19: Fire rig fire simulation

Whilst all the numerical simulations reported, irrespective of the code employed, incorporate the $k-\epsilon$ two-equation turbulence model, combustion introduces considerable additional model complexity. The SOFIE simulations of the fire event employ an eddy break-up combustion model together with radiation heat transfer calculated using the discrete transfer method. Two percent of the fuel introduced is assumed to form soot, which contributes to the radiative balance through the banded weighted-sum-of-grey-gases property model. Heat loss to the water jacket surrounding

the annulus is determined with the flowfield in a conjugate heat transfer calculation. Although the flame trajectory is captured in the simulations the peak computed mean temperatures in the fire plume are higher than measured and the predicted plume is generally narrower than observed. Figure 19 indicates peak temperatures of order 1200°C. The source of the discrepancy would appear to lie in the level of flame fluctuation, which is presently under-predicted.

2.3 Conclusion

Successful numerical flow and heat transfer simulation will permit the interaction between component and zone flow field to be defined with confidence for the first time. Positioning temperature sensitive components to take full advantage of low temperature regions of zone ventilation flow becomes possible with consequent improvements in operational reliability. With the present zone flow capability this is not possible and component temperatures can only be judged during flight testing long after the nacelle geometry has been fixed. Changes at this late stage to the nacelle are prohibitively expensive and as a consequence flows are often over specified to give large design margin with regard to temperature. This carries with it efficiency loss and fuel consumption increase. Although the application of numerical flow simulation to zone flow definition is in its infancy, confidence gained through the comparison of prediction and flow patterns generated by water analogy has been so encouraging that the optimisation of a Trent accessory zone air inlet is now being attempted. It is hoped that optimisation of the core zone exhaust will follow.

For the future the priority must be to determine the limits of geometric complexity beyond which a grid independent solution becomes impossible with current technology. This situation is of course transient and will improve with increasing computing power. Having defined an operational envelope for the numerical simulation a programme must be introduced to determine the overall accuracy of the flow prediction. Both flow and heat transfer

aspects must be considered and it is likely that in view of the very low velocities associated with zone flows that water analogy will continue to play an important role in this process. Confirmation of heat transfer capability will, ignoring radiation, be obtained by comparing the predicted wall heat transfer coefficients with that determined experimentally by heat flux meter or liquid crystal techniques. It is envisaged that this work will involve increasing theoretical and experimental complexity until acceptable zone geometry and flow simulation is achieved. To establish maximum impact on current and near-term engine designs this validation work must have clearly defined objectives and be driven against aggressive time scales.

Having determined a confidence level for the analysis technique it will then be possible to determine what level of zone component geometry simulation must be attempted in order to confirm the aerothermal performance of the zone with confidence.

3 Acknowledgements

The authors wish to thank Rolls-Royce plc for permission to publish this paper. Thanks are also due to the UK Ministry of Defence (MoD) and the UK Department of Trade and Industry (DTI) for their financial support of this work through the Defence Evaluation and Research Agency (DERA).

4 References

- [1] Lewis, MJ, Moss, JB and Rubini, PA (1997) CFD Modelling of Combustion and Heat Transfer in Compartment Fires. Fifth Int. Symp. on Fire Safety Science, IAFSS, p.463-474.